Molecular Modeling

From Virtual Tools to Real Problems

Thomas F. Kumosinski, EDITOR
U.S. Department of Agriculture

Michael N. Liebman, EDITOR
Amoco Technology Company

Developed from a symposium sponsored
by the Division of Agricultural and Food Chemistry
at the 205th National Meeting
of the American Chemical Society,
Denver, Colorado,
March 28–April 2, 1993

Chapter 22

Three-Dimensional Molecular Modeling of Bovine Caseins

Energy-Minimized Submicelle Structure Compared with Small-Angle X-ray Scattering Data

Harold M. Farrell, Jr., Thomas F. Kumosinski, and Gregory King

Eastern Regional Research Center, Agricultural Research Service, U.S. Department of Agriculture, 600 East Mermaid Lane, Philadelphia, PA 19118

To develop a molecular basis for structure-function relationships of the complex milk protein system, an energy minimized three dimensional structure of a casein submicelle was constructed consisting of one $\varkappa$-casein, four α_{s1}-casein and four β-casein molecules. The models for the individual caseins were from previously reported refined, three dimensional structures. Docking of one $\varkappa$-casein and four α_{s1}-casein molecules produced a framework structure through the interaction of two hydrophobic antiparallel sheets of $\varkappa$-casein with two small hydrophobic antiparallel sheets (residue 163-174) of two preformed α_{s1}-casein dimers. The resulting structure is approximately spherically symmetric, with a loose packing density; its external portion is composed of the hydrophilic domains of the four α_{s1}-caseins, while the central portion contains two hydrophobic cavities on either side of the $\varkappa$-casein central structure. Symmetric and asymmetric preformed dimers of β-casein formed from the interactions of C terminal β-spiral regions as a hinge point, could easily be docked into each of the two central cavities of the α-$\varkappa$-framework. This yielded two energy minimized three dimensional structures for submicellar casein, one with two symmetric β-casein dimers and one with two asymmetric dimers. These refined submicellar structures were tested by generating theoretical small-angle X-ray scattering (SAXS) curves and comparing them with experimental data. Agreement between experimental and theoretical curves was best when 120 bound water molecules were included. Comparison of SAXS data with the theoretical curves generated from X-ray data for bovine pancreatic trypsin inhibitor, by the same programs, gave similar results.

The caseins occur in bovine milk as colloidal complexes of protein and salts, commonly called casein micelles. Removal of calcium is thought to result in the dissociation of this micellar structure into noncolloidal protein complexes called submicelles (12). These submicelles consist of fourproteins, α_{s1}-, α_{s2}-, β-, and $\varkappa$-casein, in the ratios of 4:1:4:1 (8). All are phosphorylated to various extents, have an average monomer molecular weight of 23,300, and were considered to have few specific secondary structural features, such as sheets or helices (12). Recent infra-red and Raman spectroscopic data, however, have demonstrated the existence of turns and more β-sheet than expected in casein monomers and polymers (4, 5). The isolated fractions exhibit varying degrees and mechanisms of self-association, that are thought to be mostly hydrophobically driven (12, 18, 36). However, less work has been done on the tertiary and quaternary structure of these proteins in mixed associations in their native state. There is hydrodynamic evidence that, in the absence of calcium, whole casein associates to form aggregates with an apparent upper limit of 94 Å for the Stokes radius with a molecular weight of 220,000 (submicellar form) (30, 31), and this is in general agreement with the type of protein particles formed upon dissociation of casein micelles (12, 18, 36).

It has long been hypothesized that, upon the addition of calcium, these primarily hydrophobically stabilized, self-associated casein submicelles further aggregate via calcium-protein side chain salt bridges to the colloidal micelles, with a size distribution centering upon 1500 Å diameter (12, 18, 36). However, the exact supramolecular structure of the casein micelle remains unknown. Models presented have ranged from those having discrete submicelles to those having the structure of a loose porous gel (12), and to a newer model of a homogeneous sphere with a "hairy" outer layer (41). For a recent up-to-date review of micelle structure, the reader is referred to Holt (18).

To better understand the nature of the protein-protein interactions involved in micelle formation, small angle X-ray scattering experiments have been performed on whole casein in the presence and absence of calcium to mimic the micelle and submicelle structures, respectively (15, 32). It was found that micellar structures are indeed composed of submicellar particles whose structure may be approximated by an inhomogeneous spherical aggregate of two concentric electron dense regions. The inner high electron density core of the submicelle is still seven times lower than the electron density of a globular protein and has a radius of 53 Å. From these values, it was speculated that this core predominately contains hydrophobic groups. The outer loose spherical region probably contains hydrophilic groups with very low packing density. The overall radius of the spherical structure would be approximately 103 Å. From the low electron density, it was also concluded that large amounts of water could easily flow through the polypeptide chains within this structure (15, 32).

Recently, three dimensional models refined via energy minimization techniques were constructed for $\varkappa$-casein (22), α_{s1}-casein (23) and β-casein (21). These predicted structures were built from secondary structure sequence-based prediction algorithms in conjunction with global secondary structure results obtained from vibrational spectroscopy experiments (4, 5). All energy minimized structures were also in agreement with these global secondary structure determinations (21-23).

Several energy minimized aggregate structures were also presented to mimic the self-association processes for each of these caseins. In addition, qualitative speculation was presented for the interaction sites for κ-casein with α_{s1}-casein, but none were immediately obvious for κ-casein interaction sites with β-casein (21, 22).

In this paper, we will attempt to build an energy minimized submicelle structure composed of one κ-casein with four α_{s1}-caseins and four β-caseins via plausible docking sites consistent with solution physical chemical, biochemical and chemical experimental information. The energetics of all structures will be presented to ascertain if the formation of a synthetic submicelle structure, i.e., one κ-casein with four α_s-casein molecules, is the predominant intermediate or framework structure for submicelle formation. Finally, this refined structure will be compared with the geometric parameters calculated from the small angle X-ray scattering results for the submicelle particle using a variation of the procedure for computer generated models developed by Lattman (26).

Methods

Construction of Aggregate Structures

All complex aggregate structures employed the various casein monomer structures previously refined via energy minimization (21-23). Aggregates were constructed using a docking procedure on an Evans and Sutherland (St. Louis, MO) PS390 interactive computer graphics display driven by Sybyl molecular modeling software (Tripos, St. Louis, MO) on a Silicon Graphics (Mountainview, CA) W-4D35 processor. The docking procedure of this system allowed for individually manipulating the orientation of up to four molecular entities relative to one another. The desired orientations could then be frozen in space and merged into one entity for further energy minimization calculation utilizing a molecular force field. The criterion for acceptance of reasonable structures was determined by a combination of experimentally determined information and the calculation of the lowest energy for that structure.

Molecular Force Field Energy Minimization. Studies concerned with the structures and/or energetics of molecules at the atomic level require a detailed knowledge of the potential energy surface (i.e., the potential energy as a function of the atomic coordinates). For proteins, molecular mechanics methods have been used. The applications of these techniques to casein monomers have been detailed elsewhere (21-23).

Briefly in this study, the AMBER force field (44, 45) in Tripos' Sybyl software package uses electrostatic calculations which include atomic partial charges (q_i) obtained by the Kollman group (44, 45) and a united atom approach with only essential hydrogens. All molecular structures were refined with an energy minimization procedure using a conjugate gradient algorithm, in which the positions of the atoms are adjusted iteratively so as to achieve a minimum potential energy value. Energy minimization calculations were terminated when the energy difference between the current and previous iterations was less than 1 kcal/mol of protein. A nonbonded cutoff (the distance beyond which hydrogen bonding is not

considered) of 5 Å was used initially to save computer time, and then an 8 Å cutoff was used as the structures became more refined. A stabilization energy of at least -10 kcal/residue of protein was achieved for all structures, which is consistent with values obtained for energy minimized structures determined by X-ray crystallography.

Construction of Hydrated Structures. Low hydrated structures of the refined, energy-minimized casein submicelle models were constructed using a docking procedure on an Evans and Sutherland (St. Louis, MO) PS390 interactive computer graphics display driven by the Tripos Sybyl (Tripos, St. Louis, MO) molecular modeling software on a Silicon Graphics (Mountain View, CA) W-4D35 processor. The docking procedure allowed for individually manipulating the orientation of 120 energy minimized water molecules in up to four molecular display areas relative to one another. The desired orientation could then be frozen in space and merged into one molecular display area for energy minimization calculation using a molecular force field. The criterion for acceptance of reasonably hydrated structures was determined by a combination of experimentally determined information, i.e., DNMR relaxation results (13, 15) in combination with the calculation of the lowest energy for that structure. All water molecules with unacceptable van der Waals interactions were eliminated.

For hydrated structures with large amounts of water, the Tripos (St. Louis, MO) "Droplet" algorithm was employed. This procedure creates a monomolecular layer of water around an entire structure in an objective manner. In these calculations, a structure with a low hydration value (120 water molecules) was created using the above docking procedure, then the high hydration model was generated using the "Droplet" algorithm. Thus, a total of 2723 water molecules could be objectively added to the low hydrated structure yielding a total hydration value of 0.244 g water/g protein.

Calculation of SAXS Profiles. All small-angle X-ray scattering profiles were calculated for the unhydrated and hydrated structures using a computer program based on an algorithm developed by Lattman (26). This methodology not only allows for rapid calculation of SAXS profiles, i.e., at least ten times faster than other procedures, but also allows for optimization of the residual between calculated and experimental SAXS profiles using adjustable temperature factors for protein, bound water and solvent water. The effects of solvent have been modeled by subtracting from each protein atom a properly weighted solvent water molecule. Protein hydrogen atoms are implicitly accounted for using the strategy of Gelin and Karplus (6).

The scattering profile is given by

$$I(R) = \tfrac{1}{2} \sum_{n=0}^{x} \sum_{m=0}^{n} \epsilon_m N_{m,n} |G_{m,n}(R)|^2 \qquad (1)$$

where

$$G_{m,n}(R) \sum_j F_j Y_{m,n}(\theta_j, \phi_j) j_n(2\pi r_j R) \quad (2)$$

I is the scattering intensity, and R = 2 sin θ/λ where θ is the scattering angle and λ is the wavelength of incident radiation. N is the number of atoms and ϵ is a constant related to the order (n or m) of the LeGendre polynomial used. $Y_{m,n}$ are complex spherical harmonics, j_n are the spherical Bessel functions. The index j runs over all atoms, i.e., protein, protein-bound water and solvent water, and r, θ and ϕ are their corresponding spherical atomic coordinates. The expanded structure factor, F_j is given by the following:

$$F_j = (\alpha_P f_P + \alpha_B f_B - \alpha_W f_W) \exp(2\pi i r_j R) \quad (3)$$

where α_P, α_B and α_W are the occupancies of the protein atoms, bound water and solvent water, respectively. The temperature factors, B, are related to the structure factors by

$$f_P = f_P^0 e^{-B_P} \quad (4a)$$

$$f_{BW} = f_{BN}^0 e^{-B_B} \quad (4b)$$

and

$$f_W = f_W^0 e^{-B_W} \quad (4c)$$

where the f^0 are the structure factors in the absence of thermally induced vibrational motion and the B factor compensates for temperature induced changes (a Debye-Waller constant). All subscripts of P, B and W represent the atoms due to the protein, bound water and solvent water. The units of B are $Å^2$.

All calculations using the Lattman program were performed on a VAX 8350 (Digital Equipment, Waterbury, MA) computer. All BPTI calculations took 20 min. to complete whereas submicelle structures required at least 22 hrs.

Results and Discussion

Refined Casein Complex Structures

Synthetic Submicelle: Framework. Following the discovery by Waugh and von Hippel (42) of κ-casein, the stabilizing factor of casein micelles, many studies aimed at understanding the nature of the protein-protein interactions involved were conducted. For the bovine system, these studies focused upon reconstituting micelles with mixtures of α_{s1}- and κ-caseins (28, 35). The reasons for this selection included:

1. Synthetic micelles roughly resembling those of parent micelles could be formed from these two fractions alone.

2. Historically, β-casein was readily separable from the other fractions by mild procedures, so that it was not considered a primary reactant.

3. Separation of κ-casein from the α-complex had been a relatively difficult task, indicating a high degree of interaction.

All of these factors pointed toward the importance of α_{s1}- κ-casein interactions in the bovine casein system (20, 28, 35).

Initial micelle reconstitution experiments (42) suggested that maximum stability of reformed micelles occurred at a ratio of 4:1, α_{s1}-:κ-casein. Later, Noble and Waugh (28) suggested a ratio of 10:1 overall but with stronger 1:1 complexes as nucleating sites. In consideration of these studies three factors are important: first, these were whole κ-casein fractions and Groves et al. (17) have recently shown that these preparations contain polymers ranging up to octamers and above as well as some monomers, depending upon the degree of disulfide bonding; secondly, the ratio of 4:1:4:1 for α_{s1}-:α_{s2}-:β-:κ-casein, is about 9:1 in terms of phosphorylated calcium sensitive caseins to κ-casein; finally, the redox potential of the bovine mammary gland lies far toward the reducing end of the scale as the ratio of NADP to NADPH is 4×10^{-5} (2). All of these factors considered, along with the potential reactivity of κ-casein as a monomer (46), a ratio of 4:1 for the interaction of α_{s1}-casein with a reduced κ-casein monomer appeared to be a logical starting point for the construction of a theoretical submicelle.

Figures 1(a), (b) and (c) show the backbone structures for the energy minimized models of κ-casein B, α_{s1}-casein B and β-casein A^2, respectively. The κ-casein structure which has been colloquially referred to as a "horse and rider" model (Figure 1(a)) contains two sets of "dog-leg" structures. These so-called "dog-leg" structures are the result of two sets of antiparallel sheet structures each connected via a proline residue in a γ-turn configuration, i.e., prolines 27 and 47. It may be noted that for κ-casein, these prolines and the preceding and following sequences appear to be functionally preserved across a variety of species whose primary structures are known (19, 23). Hydrophobic groups, notably tyrosine and valine which are evolutionarily conserved, are the predominant side chains located on both the smaller "dog-leg" (residues 20-34) and the larger one, (residues 39-55). In addition, each "dog-leg" contains a lysine side chain near the pivotal proline residue; there is conservation of these positive charges in almost all κ-caseins (19, 23). This positive charge could conceivably form hydrophobically stabilized ion pairs with another "dog-leg" structure from another casein containing an acidic group in a similar position. Such "dog-leg" structures could easily be docked in an antiparallel fashion to maximize attractive dipole-dipole interactions and yield an acceptable stabilization energy.

Inspection of the β-casein A^2 structure of Figure 1(c) shows no such "dog-leg" structures. Only two distorted arm structures are observed; but, these arm structures contain hydrophilic side chains, and are unlikely candidates for hydrophobic interaction with κ-casein. The hydrophobic domain, left side of

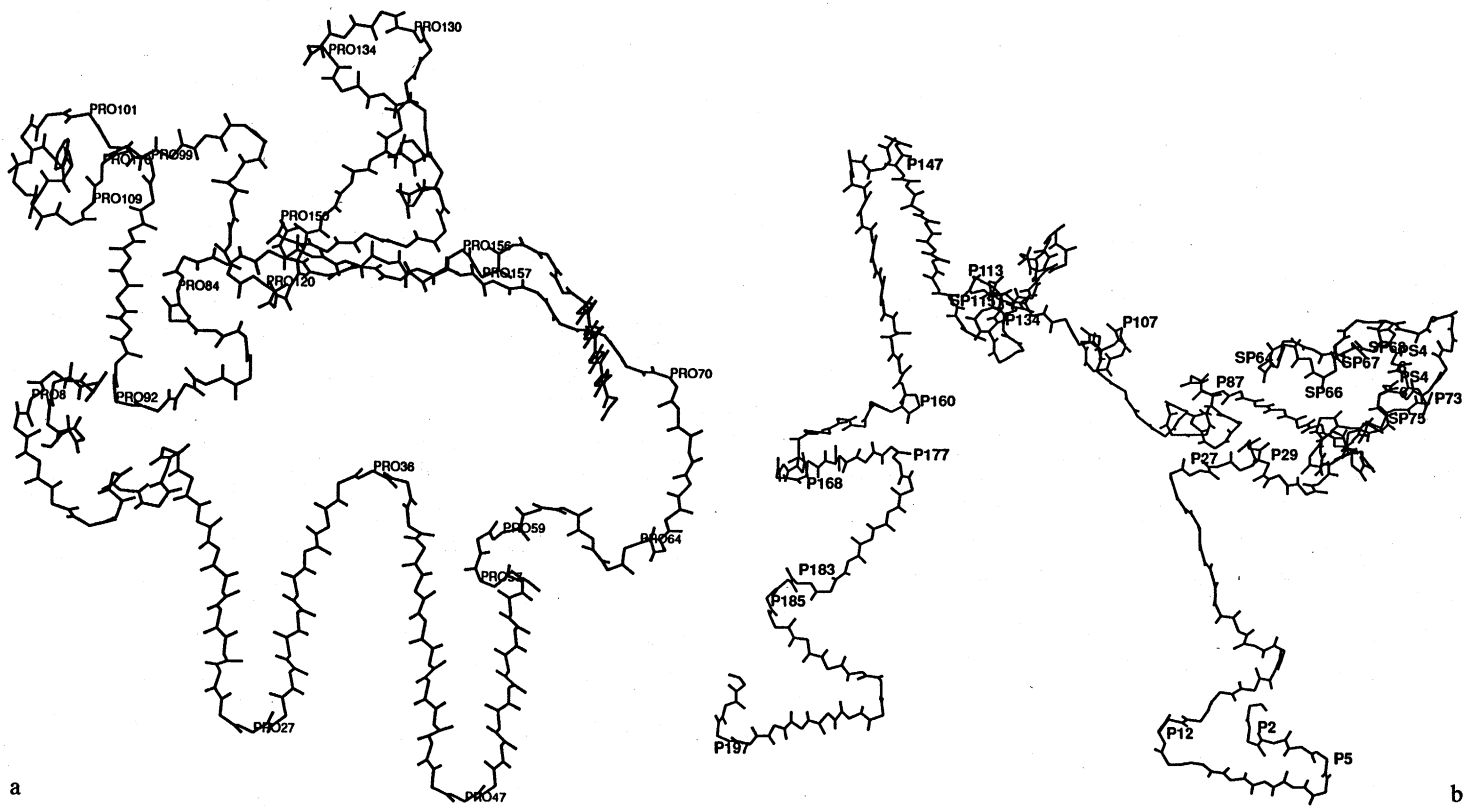

Figure 1a and 1b. (a) Backbone structure with labeled prolines (PRO) of χ-casein B. (b) Backbone structure with labeled prolines (P) and phosphoserines (SP) of α_{s1}-casein B. (Figure 1a reproduced with permission from reference 22. Copyright 1993 American Dairy Science Assocation.)

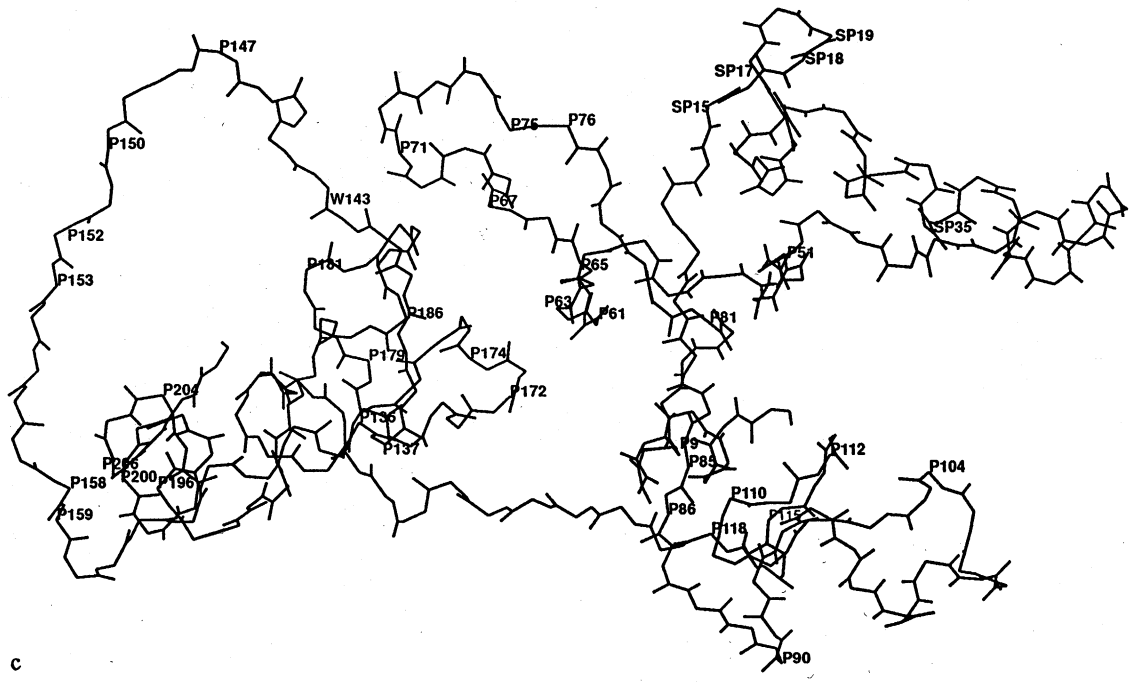

c

Figure 1c. Backbone structure with labeled prolines (P) and phosphoserines (SP) of β-casein A^2. (Reproduced with permission from reference 22. Copyright 1993 American Dairy Science Assocation.)

Figure 1(b), of the α_{s1}-casein B structure however has two such "dog-leg" structures, i.e., a large one, residues 136-159, and a smaller one, residues 162-175, whose side chains are predominantly hydrophobic. Both of these "dog-leg" structures contain proline residues, i.e., residues 147 and 168, as pivotal points for the stranded antiparallel sheet structures. Unlike the γ-turn structures in κ-casein, these prolines are in the 2 position of a β-turn configuration, allowing for greater intra-chain hydrogen bonding. The larger structure, residues 136 to 159 with a pivotal proline at residue 147, appears to have been deleted in ovine α_{s1}-casein, but is functionally conserved in rat at n+3 residues from bovine (19, 23). The larger "dog-leg" thus has some variance in charge and size across species. In contrast, the smaller "dog-leg" centering on proline 168 is functionally preserved in all species of α_{s1}-casein molecules examined, as is the proline at 160 which begins this structure (19, 23). Additionally, tryptophan 164 and tyrosine 166 are invariant and may potentiate hydrophobic interactions. There are no positive charges preceding the pivotal proline but a negatively charged aspartic 175 is conserved following this residue (19, 23).

In a previous report, it was shown that the large "dog-leg" structure, residues 136-159, of α_{s1}-casein B was an excellent site of dimerization of α_{s1}-casein, yielding an interaction energy of -505 kcal/mole, as calculated from the resulting difference between the energy of the dimer (Col. 2 of Table 1) and two times the energy of the monomer (Col. 1 of Table 1). As noted above, variance across species in this region has led to the prediction that ovine α_{s1}-casein may have altered self-association properties relative to its caprine and bovine counterparts (23). Dimer formation (see Figure 2(a)) at the larger "dog-leg" permits the easy docking of one of the small α_{s1}-"dog-leg" structures (residues 162-175) in an antiparallel fashion to a κ-casein "dog-leg" structure. In fact, the last residue of the small α_{s1}-casein "dog-leg", aspartic 175, would easily interact with either lysine residue (24 or 46) on each of the "dog-leg" structures of κ-casein, resulting in a hydrophobically stabilized ion pair formation. The choice of α_{s1}-casein interacting as a dimer is supported by the studies of van de Vroot et al. (39) who examined the interactions of whole κ-casein and α_{s1}-casein by sedimentation equilibrium. They suggested dimer formation by α_{s1}- could precede α_{s1}- κ-interactions. Furthermore, they demonstrated that κ-κ-polymers were larger in size than the resultant α_{s1}-κ-complexes, indicating a more energetically favorable state for the complexes. Pepper (30) and Pepper and Farrell (31) showed similar changes by gel chromatography. Slattery and Evard (37) observed complex formation between reduced κ-casein and α_{s1}-casein by sedimentation velocity studies. Association constants at 20°C for α_{s1}- and κ-casein complexes range from 2 to 8 x 10^4 M^{-1} (K_D = 12 to 50 μM) depending upon the method of measurement (39). For the polymerization of reduced κ-casein to its "micellar" complex an association constant of 4.5 x 10^4 M^{-1} (K_D = 22 μM) can be calculated from Vreeman et al. (40). Association constants for α_{s1}-casein polymerization range from 8 to 11 x 10^4 M^{-1} (K_D = 9 to 12 μM) as calculated from Schmidt and Payens (35) at 21°C and ionic strength equal to .1. Thus, considering the evidence for complex formation and the similarity of the association constants, there is a very high probability that α_{s1}- κ-caseins could form these postulated mixed complexes.

Table 1. Calculated energy of α_{s1}-casein and β-casein dimers

Structure	α_{s1}-Monomer	α_{s1}-Dimer	β-Casein Dimer
Bond Stretching	34.3	75.7	82.5
Angle Bending	425.5	892.9	1314.5
Torsional	427.3	840.9	44.6
Out of Plane Bending	15.6	36.6	602.6
1-4 van der Waals	305.9	616.3	1091.6
van der Waals	-872.4	-1805.0	-2094.2
1-4 Electrostatic	2135.3	4268.2	4400.1
Electrostatic	-4426.3	-9337.6	-10230.0
H-Bond	-46.7	-96.4	-123.8
Total	-2001.6	-4508.5	-4912.1

Docking two α_{s1}-casein dimer structures via their small "dog-leg" structures in an antiparallel fashion with the two "dog-leg" structures of κ-casein, one interaction in front of the κ-casein (hydrophilic ends up) and one behind the other "dog-leg" structure (hydrophilic ends down), yielded a rather spherically symmetric structure. Energy minimization of this model composed of one κ- with four α_{s1}-casein monomers yielded an excellent energy of -11811.1 kcal/mol as seen in Col. 1 of Table 2. The architecture of this refined synthetic submicelle structure is presented in Figure 3 as a ribboned backbone structure.

Here, all the hydrophilic domains of α_{s1}-casein which contain the serine phosphates (pictured as ball and stick models) and acidic groups, are located on the outside of the structure for easy access by water and calcium as potential sites for calcium binding and cross-linking which leads to micelle formation. The dimeric phosphate clusters are however diagonal (left to right) from each other decreasing charge repulsions. The internal portion of this structure is divided into four open sectors. The two parallel to the κ-casein central structure (top view of Figure 3) are largely hydrophobic in which fats and other hydrophobic solutes could bind. The other two quarters, which are perpendicular to the κ-casein (left and right of 3, are hydrophilic and are easily water and enzyme accessible. The massive hydrophobic surface area produced by the two central hydrophobic quadrants (Figure 3) can also be potential interaction sites for four β-casein structures via hydrophobic interactions provided the area is large enough not to cause poor van der Waals contacts. It should also be noted at this time, that the docking of four α_{s1}-casein structures to the κ-casein structures could not be accomplished by use of any of their larger "dog-leg" structures without producing large positive

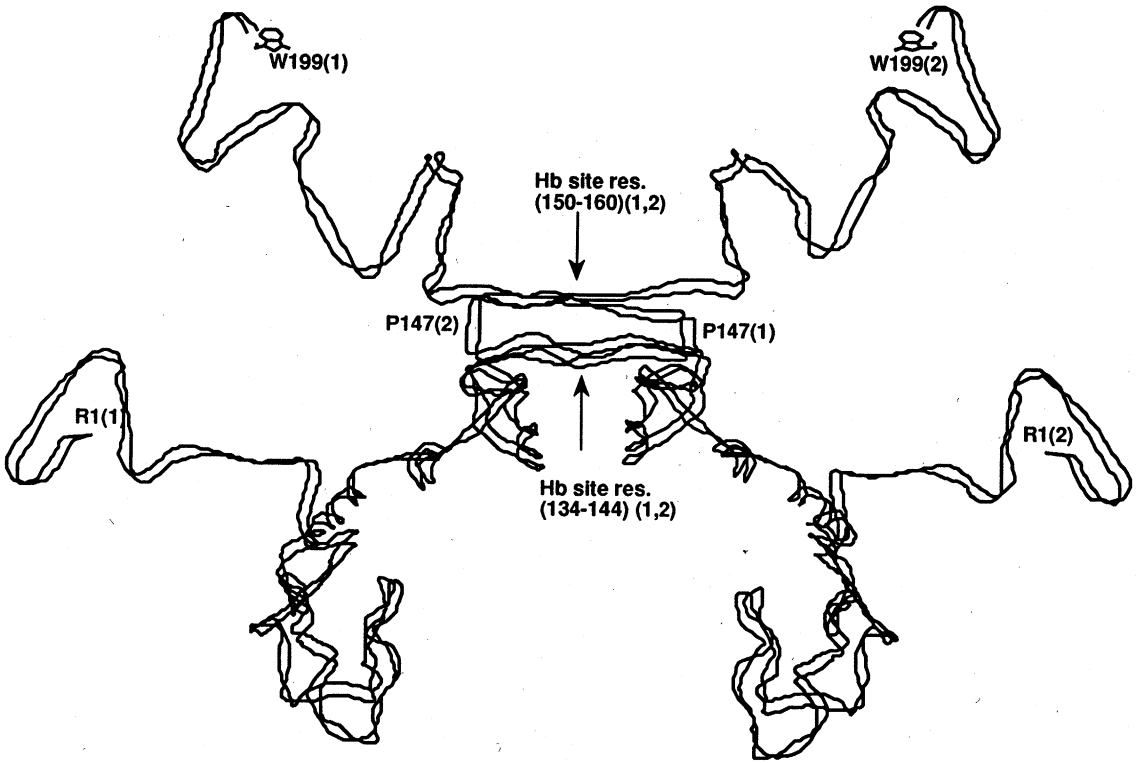

Figure 2. (a) Double ribbon structure of α_{s1}-casein B dimer constructed by docking two large hydrophobic sheets in an antiparallel fashion interactions sites noted (1,2 refer to molecules 1 and 2). Hb = hydrophobic sitem, W199 = C-terminal tryptophan, R1 = N-terminal arginine, P147 = proline 147.

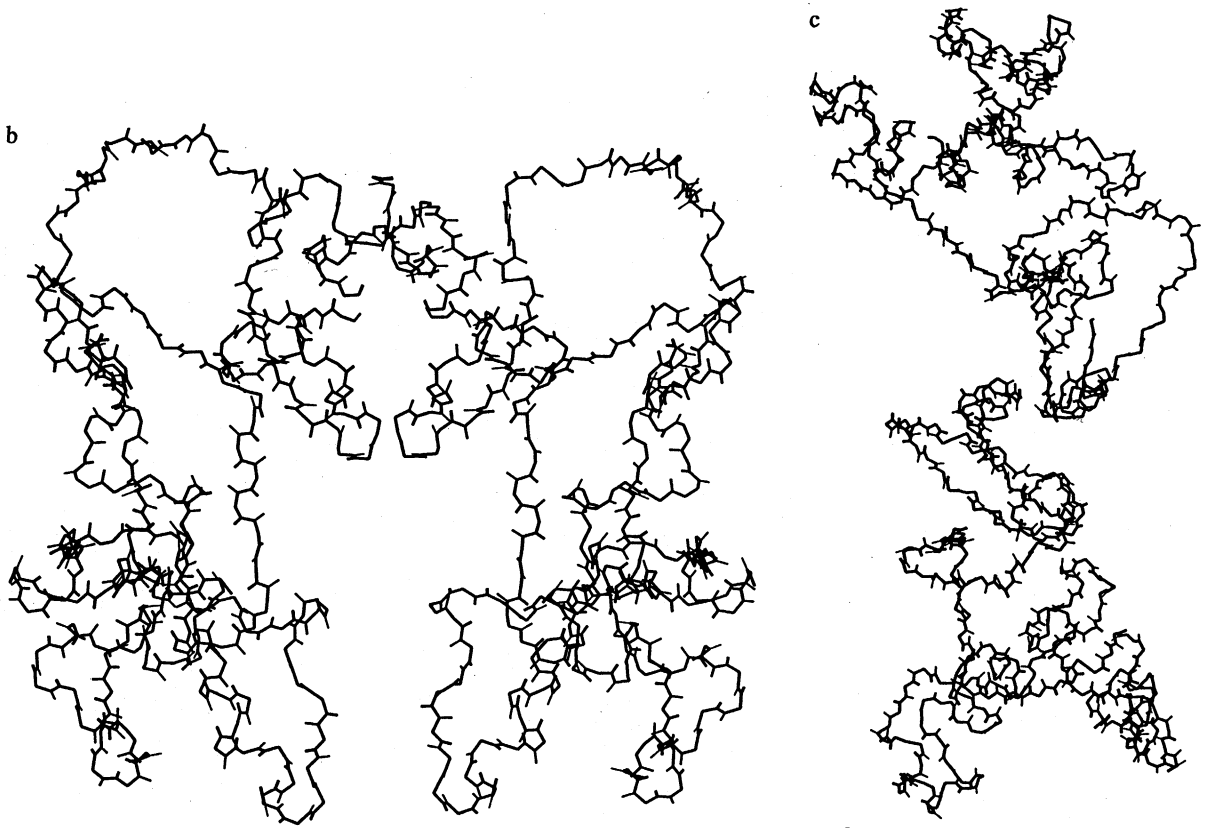

Figure 2. Continued. (b) Backbone structure for β-casein A^2 asymmetric dimer. (c) Backbone structure for β-casein A^2 symmetric dimer.

Table 2. Energy for refined casein submicelle structures

Structure	Syn. Sub.[1]	Submicelle[2]	
		Asym.	Sym.
Bond Stretching Energy :	177.7	208.7	363.2
Angle Bending Energy :	2280.1	4909.0	3430.1
Torsional Energy :	1996.4	2888.4	3272.6
Out of Plane Bending Energy :	93.1	200.5	496.1
1-4 van der Waals Energy :	1311.5	2697.3	2939.1
van der Walls Energy :	-4003.7	-8379.8	-8200.5
1-4 Electrostatic Energy :	12046.8	19000.7	19292.8
Electrostatic Energy :	-25454.9	-43813.0	-45120.4
H-Bond Energy :	-258.1	-513.9	-519.0
Total Energy :	-11811.1	-21802.2	-24047.0

[1] Syn. Sub = synthetic micelle framework of one κ-casein and two α_{s1}-casein dimers.

[2] Submicelle = theoretical submicelle, consisting of the one κ-casein and two α_{s1}-casein dimer framework with two β-casein dimers added in asymmetric or symmetric fashion.

destabilization energies, caused initially by poor van der Waals contacts. This (Figure 3) is the best structure yielding the lowest energy as determined by up to 10 to 15 docking combinations between two α_{s1}-dimers and one κ-casein monomer.

From the above rationale, it appears on the basis of experimental evidence and from modeling considerations that before the complete casein submicelle can form, a synthetic submicelle framework consisting of κ-casein with α_{s1}-casein structures could form as an energetically favorable intermediate. After this structure is formed, β-casein can then interact to form a hypothetical casein submicelle.

Submicelle Structure. As the interaction of β-casein with the micelle is primarily hydrophobic (18, 34, 43) it seemed plausible to dock two β-caseins within each of the two larger hydrophobic quadrants of the refined synthetic submicelle structure which occur to the right and left of the "rider" (see Figure 3). However, whether this should be performed in a random fashion was not immediately evident.

In a previous report, the energy minimized structure of β-casein monomer and aggregates were presented (21). A radius of gyration of 23 Å could be calculated for the monomer model which can be approximated by a prolate ellipsoid of revolution of radii 42 Å by 21 Å. It resembles a detergent molecule in as much as one end of the molecule contains two hydrophilic arms while the other end and central portion of the structure contains predominantly hydrophobic side chains. To comply with chymosin cleavage experiments of Creamer (7), an asymmetric dimer was constructed as a precursor to β-casein polymeric structures (21). (The terms symmetric and asymmetric will be used here to describe structures with and

Reprinted from ACS Symposium Series No. 576
Molecular Modeling: From Virtual Tools to Real Problems
Thomas F. Kumosinski and Michael N. Liebman, Editors
Published 1994 by the American Chemical Society

without a center of inversion, respectively.) The asymmetric dimer was constructed in an antiparallel fashion with a β-spiral region of residues 190-206 used as a hinge point; the importance of this region in β-casein interactions has been established by Beery and Creamer (3). In the resulting dimer, all the hydrophilic groups remain on one side of the structure and the hydrophobic groups are located on the other side (Figure 2(b)). After energy minimization this dimeric structure yields a total energy of -4912.1 kcal/mole (Col. 3 of Table 1). Two of these β-casein A^2 dimers were then docked in an asymmetric fashion within the two hydrophobic quadrants of the synthetic submicelle framework structure of Figure 3, with their hydrophilic arms pointed outward from the central cavity. This resulting structure (Color Plate 20) was next energy minimized and yielded an acceptable energy of over -10 kcal/mole/residue (Table 2). Although no stabilization energy is observed, such a structure is highly likely since the interaction between the β-casein dimers and the synthetic submicelle structure is for the most part hydrophobic, which is supported by the dissociation of β-casein from submicelles and micelles at 4°C and below (1, 9, 10, 34).

Another submicellar structure, which will be referred to as a symmetric model, can be built by the symmetric docking of two β-casein A^2 symmetric dimers into the two hydrophobic cavities of the synthetic submicelle structure. The β-casein A^2 symmetric dimer (Figure 2(c)), contains two hydrophilic sites at either end of the structure and a central hydrophobic region. The symmetric dimer has no loss in stabilization energy and after minimization gives a total energy of -5484.4 kcal/mole, which is different from the asymmetric dimer and will be discussed in detail in the energetics section of this manuscript. In this submicelle structure, the symmetric dimers must be docked with their central hydrophobic portion in contact with the hydrophobic cavity of the synthetic submicelle structure so that their hydrophilic areas are actually perpendicular to corresponding β-casein dimeric structures docked within the asymmetric submicellar model (Color Plate 20). The resulting structure was energy minimized (Table 2) and is presented in Plate 20. It should be noted that one of the β-casein hydrophilic portions of the symmetric dimer partially covers the view of the GMP of the κ-casein within this structure, but it in no way interferes with access of the chymosin to the phenylalanine-methionine cleavage site of κ-casein, nor does it hinder access to glycosylation sites on the κ-casein.

Several other approaches to docking β-casein dimers were attempted. Most of these resulted in extreme loss of stabilization energy. The dominating factor in docking the four β-caseins is the proximity of the four hydrophilic ends to each other and to the phosphate rich portions of α_{s1}-casein. Charge repulsions in these areas prevent many hypothetical approaches. To test the above energy minimized structures, comparisons of the models will be made with experimental evidence derived from Raman spectroscopy and small-angle X-ray scattering.

Secondary Structural Analysis. Global secondary structural analysis was initiated on the energy minimized three dimensional submicelle structures. The results were compared with the reported global secondary structure calculated from Raman spectroscopy (Table 3). No significant changes in the ϕ, ψ angles of the backbone peptide bonds between the individually refined κ-, α_{s1}- and β-casein structures and

Figure 3. Refined structure of casein synthetic submicelle framework, i.e., one $\varkappa$-casein B and four α_{s1}-casein B monomers. Ribbon backbone; for α_{s1}-casein monomers (Figure 1b) side chains of serine phosphates only are shown as ball and stick models. The view is from the top in which $\varkappa$-casein (see Figure 1a) can be seen as essential nucleation point for the formation of this framework structure.

Table 3. Comparison of initial structures with spectroscopic data

Sample		% Helix	% β-Structure	% Turns	% unspec
Submicelle (Lyophilized)	Raman[1]	8 - 18	24 - 30	36 - 39	16 - 32
$\varkappa$-casein	Refined	16	27	30	26
α_{s1}-casein	Refined	8	18	34	40
β-casein	Refined	10	20	34	36
Submicelle[2]	Calculated	10	20	34	36

[1]References 4, 5.
[2]Constructed for asymmetric and symmetric models (see text).

those within the two submicelle structures was observed. Table 3 also contains the secondary structure analysis calculated in previous communications for the individual casein structures. Hence, an average of the molecular fractions of caseins in the submicelle could be used to calculate the global secondary structure of the submicelle structure. The results of this calculation are given in Table 3 as the Calculated Submicelle row and is in reasonable agreement with the experimentally determined values from Raman spectroscopy (Row one of Table 3), even though the Raman spectroscopy experiments were performed on a lyophilized powder of whole sodium caseinate. It is hoped that in the future, precise global secondary experiments will be performed in solution using Raman or FTIR spectroscopy because this same Raman study (5) showed that conformational changes can occur in β-casein A^2 during lyophilization. While this type of analysis does not prove the refined submicelle structure, it does add further validation to the possibility of such a refined model. It should be stressed, however, that molecular dynamic calculations should be performed in the future, for it is the dynamic structure which ultimately should be correlated with solution physical chemical properties.

Comparison with Solution Structural Results. The energy minimized three dimensional models of the casein asymmetric and symmetric submicelles, shown in (Color Plate 20), can all easily be approximated by a spherical particle of two packing densities. The distance from one end of the β-casein through the $\varkappa$-casein structure and to the end of the opposite β-casein molecule is 100 Å in both models. The packing density of this region would be considered higher than any other within the overall structure. The longest distance measured from one α_{s1}-casein hydrophilic domain to an opposite one is about 200 Å. These values, symmetry and packing densities, agree qualitatively with recent small angle X-ray scattering results (15, 32). Here, the data were modelled as an inhomogeneous sphere of two electron densities of diameter 106 Å by 203 Å with the same center of symmetry. In addition, the low electron density is consistent with the low packing density observed in the refined structure. Such a low electron density could be interpreted as a high hydration value or a particle in which water can easily flow throughout the polypeptide chain or both.

From our present structural study it would be reasonable to assume that the hydrophilic domains of α_{s1}-casein B within the synthetic submicelle structure (Figure 3(b)) are potential interaction sites for colloid formation by self-association of the synthetic submicelle structure via calcium salt bridges. Such a colloidal matrix structure could easily allow for the temperature induced hydrophobic association or disassociation of β-casein from that colloidal matrix structure. In fact the remnant after cold dissociation would mimic the micelle framework postulated by Lin et al. (27). It should be noted that the above is not a conclusive proof for the mechanism of submicelle and micelle formation. It is a working hypothesis, as is the structure, and is in need of a large amount of quantitative experiments to disprove, prove or further refine this structure and mechanism. As with all such models it is not an end in itself but a spring-board to further research.

Many studies of several investigators (12, 18, 35) show that casein submicelles have a significantly higher hydration value than for globular proteins, i.e., 3-6 g

water/g protein. Quantitative comparison of this submicelle structure with small angle X-ray scattering results required the development of a methodology suitable for assessing differences in the models as well as the effects of added water.

Bovine Pancreatic Trypsin Inhibitor. To test the programs developed for comparison of energy minimized structures with SAXS profiles for hydrated and unhydrated casein submicellar structures, and to more fully understand the parameters calculated from the Lattman program, it was important to first use the procedure on a protein molecule with a known hydrated three dimensional X-ray crystallographic structure. We followed the lead of the Lattman paper (26) and used the X-ray and neutron crystallographic structure of BPTI, i.e., the 5BPTI file in the Brookhaven protein databank. The structure obtained in the protein data bank consists of all protein hydrogens as well as 63 water molecules with hydrogens and one bound anion. To mimic the Lattman calculation to be used on the casein models, all hydrogens were removed, the anion was eliminated as well as the three waters associated with this anion. This structure was presented to the Lattman program using the scattering data provided in the program files which were originally determined by Pickover and Engelman (33). To be consistent with the calculation of submicellar casein, only 20 equally spaced data points were used. The resulting calculated B values for the protein, B_P, the bound water, B_B, and the solvent water, B_W, as well as the residual (the variance of the calculated data from experimental data) as a measure of the goodness-of-fit, are presented in the first row of Table 4. The overall profile of the calculated and experimental SAXS results, as filled triangles with a connecting line, are shown in Figure 4(a). As seen in Figure 4(a), the fit of the structure to the SAXS data is acceptable; even the residual value of 0.220 (Table 4) represents an error of only 3 percent. The B values for the bound water and solvent are in reasonable agreement with those calculated by Lattman (26), i.e., 59 $Å^2$ and 72 $Å^2$, respectively; however, the B_P of 125 $Å^2$ is much lower than that presented in his paper, i.e., 284 $Å^2$. Presumably, this discrepancy may be caused by the use of a lower number of experimental data points. Since the casein submicelle models, developed above, initially contained no water and were energy minimized, it was decided to first test the effect of energy minimization on the goodness-of-fit with experimental SAXS profiles using the Lattman procedure. Energy minimization of the BPTI structure with 60 water molecules from X-ray crystallography, resulted in an energy of -1712.8 kcal, which is well below the energy criterion of -10kcal per residue or water molecule, i.e., -118 kcal/mole, that we have previously chosen to impose as an acceptable criterion for improvement in the energy value (21-23). The resulting energy minimized structure was then presented without hydrogen to the Lattman program and the resulting B and R values are given in row 2 of Table 4. The residual, R, value of 0.160 for the refined structure is somewhat lower than that of the unrefined model while their corresponding B_P and B_B values are much higher. $B_P = 224$ actually approaches the value of 284 found by Lattman (26). The reasons for the better fit of the energy minimized over the initial structure with the experimental SAXS profiles are not clear at this time. However, since the unrefined structure was determined in the crystal state and the SAXS profiles are obtained in solution where dynamic processes occur, a hypothesis concerning the

Table 4. Temperature factors for bovine pancreatic trypsin inhibitor (BPTI) from SAXS*

Refined	Waters	B_P [1]	B_W [2]	B_B [3]	R [4]
No	60	125	55	89	0.220
Yes	60	224	58	200	0.160
No	0	-48	-45	—	0.186
Yes	0	-18	-60	—	0.133
No	4	-12	-47	102	0.0833
Yes	4	-3	-41	122	0.0731
Yes	202	137	120	35	0.148

*SAXS—Small Angle X-ray Scattering.
[1]B^P—Temperature factor for protein, Å^2.
[2]B_W—Temperature factor for free water, Å^2.
[3]B_B—Temperature factor for bound water, Å^2.
[4]R—Residual: deviation of calculated from experimental SAXS data.

necessity of a protein adapting to a lower possible energy structure in solution may be offered.

This hypothesis can be tested at this time by using, the Lattman program, together with theoretical unhydrated and hydrated forms of BPTI in their original and energy minimized structures. Here, the refined and original structures of BPTI with all waters eliminated and with only 4 internal waters retained can be used to calculate theoretical SAXS profiles (Table 4). In addition, calculated energies for the refined structures of BPTI containing no waters and four internal waters are shown in Table 5. The results of the Lattman program for the initial and refined structures with 0 and 4 waters are listed in rows three to six of Table 4. All temperature factors for the protein, B_P, are negative (Table 4). Thus, no physical interpretation regarding the vibrational motion of atoms of the protein can be made. It appears that energy minimization of structures always improves the goodness-of-fit between theoretical and experimentally determined SAXS profiles when using the Lattman methodology and the Tripos software. Comparison can be made for the variation of hydration levels versus goodness of fit to SAXS (R values) for only the energy minimized structures of the BPTI. The results of the correlation of experimental and theoretical SAXS profiles for the refined unhydrated and various hydrated structures of BPTI are given in rows 2, 4, 6 and 7 of Table 4. The lowest value of the residual, R, between the experimental and theoretical SAXS profiles is obtained for the refined structure of BPTI with four bound internal waters. The fit of the theoretical SAXS profile for the structure is presented in Figure 4(a) as open circles; this structure is depicted in Figure 4(b). Comparison

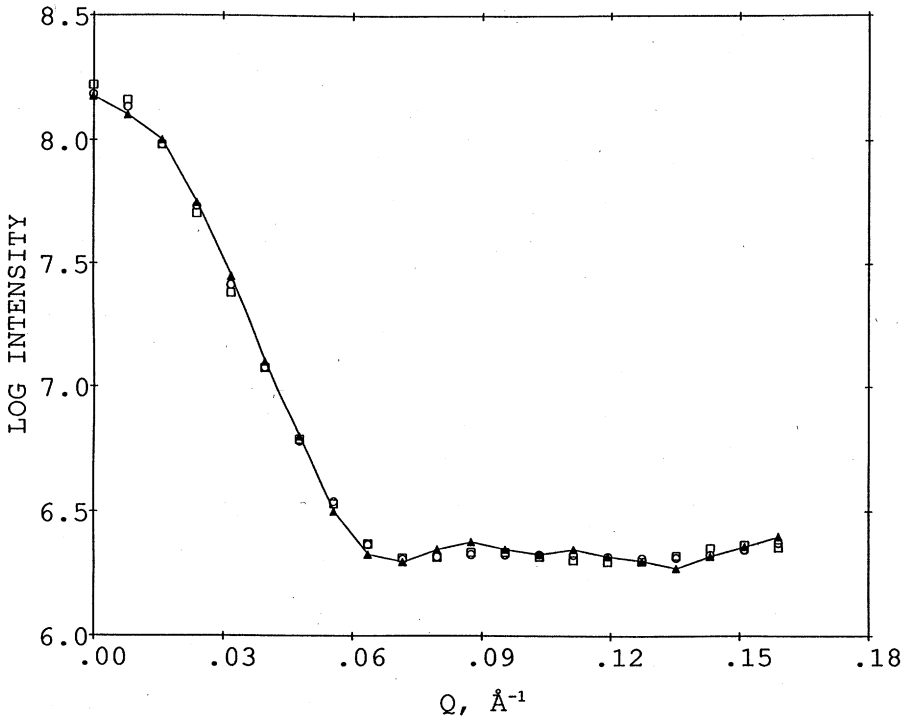

Figure 4. (a) SAXS profiles of Bovine Pancreatic Trypsin Inhibitor, BPTI: filled triangle with connecting lines, experimental data (33); squares, optimized theoretical curve from X-ray crystallographic structure with 60 waters determined via neutron diffraction; circles, optimized theoretical curve from energy minimized structure with 4 internal waters.

with the 60 water BPTI structure, depicted as squares in Figure 4(a) with the four water structure (open circles) and the experimental data (filled triangles) show only slight differences at high Q values but deviate mostly at the very low Q values where the radius of gyration and molecular weight are calculated. Overall, even the 60 water structure profile shows a satisfactory fit between theoretical and experimental SAXS profiles even though its R value is three times larger than the refined internally bound water BPTI structure (Table 4). However, since the B value of the protein is negative for the four internally bound water BPTI structure, we would conclude that some more bound waters are necessary for proper simulation of the data. Using the 202 water structure yields a more acceptable value of 137 $Å^2$ for the B_P value as well as a positive B_W value, but with an increase in the R value by a factor of two. Here the actual number of water molecules that should be added to the protein surface appears to be somewhere between 0 and 198. Lattman (26), as well as other investigators (29) using NMR

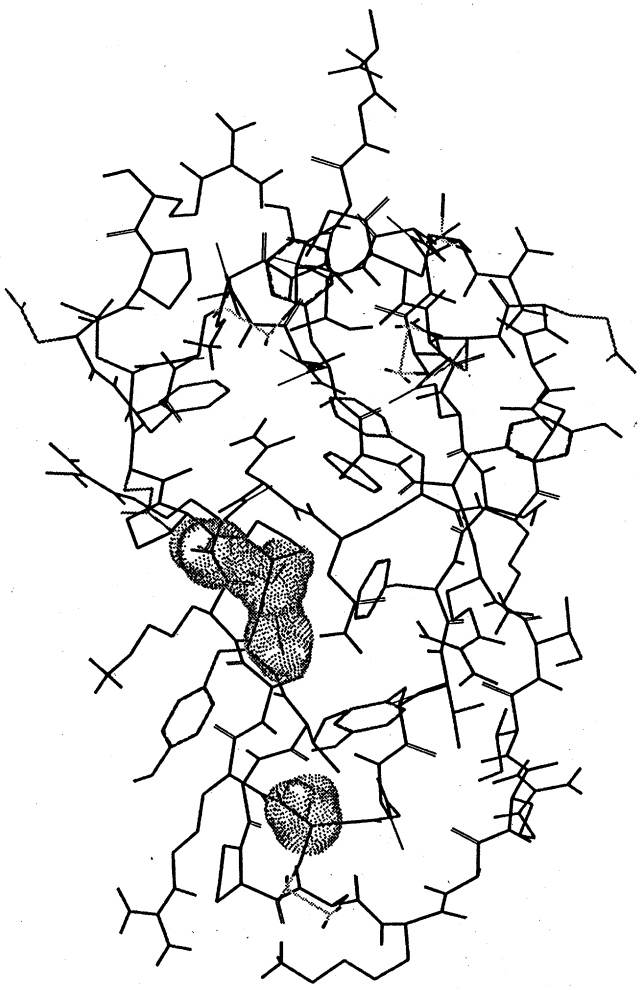

Figure 4. (b) Structure of BPTI with 4 internal waters. The structure shows both backbone and all side chains, as well as van der Waals dot surface (gray) of 4 internal waters.

experiments, also concluded that at least four but no more than ten water molecules, six by NMR, are bound to BPTI. The obvious problem of the number of water molecules, four to ten, bound to BPTI and the exact location of the other two to six surface waters does not allow us to further test their methodology using the SAXS profiles of BPTI. However, the results so far indicate that the method of Lattman is still useful for determining whether or not an energy minimized three dimensional structure can be tested by generation of theoretical SAXS profile results and comparing these with experimental data to determine if structures contain bound waters, externally or internally, when they exist in solution.

Bovine Casein Submicelle Structure. We now turn our attention to attempt to test the energy-minimized casein submicelle structures using the Lattman methodology with published experimental SAXS profiles following the methodology developed for BPTI. We will also attempt to ascertain the need for and location of bound waters within the structures. A search of the literature showed two papers (24, 38) in which the SAXS data were in graphical form for computer aided digitalization, and the appropriate conditions were used to insure submicellar (maximally aggregated) casein solution structure. However, one of the papers (38) only contained SANS data in D_2O and, even though contrast variation experiments were performed at several H_2O/D_2O mixtures, no molecular weights were calculated. Only one report exists whereby precise SAXS experimental profiles were obtained in H_2O and not in D_2O where hydrophobic protein self-association would be increased (24). Also in this study, molecular weights were given with statistical errors calculated to insure that submicellar casein was present. No variation in molecular weight was observed with respect to protein concentration insuring the elimination of particle polydispersity. However, whole casein was used for this SAXS study which contains 10 percent of α_{s2}-casein (8) and as noted above no α_{s2}-casein structure exists within this predicted three dimensional submicellar model. Nevertheless, since only 10 percent of the submicelle casein particle contains α_{s2}-casein, it is thought that comparison of the theoretical curves from the submicelle structure and the experimental SAXS profiles would still lead to fruitful results.

Without energy minimization, both the asymmetric and symmetric unhydrated submicelle structures were subjected to the Lattman procedure for comparison with experimental SAXS profiles. The comparisons with experimental results are presented in Figure 5(a). Here, the experimental data are shown as filled triangles with connecting lines while the theoretical curves, using the asymmetric and symmetric structures, are represented by circles and squares, respectively. As can be seen, both structures yield rather unfavorable SAX profiles. While agreement with experimental data is moderate at large Q values, disagreement is unacceptable at low values which would yield erroneous calculated molecular weights and radii of gyration. The Lattman temperature parameters (B values) from these calculations are given in Table 5. The B values for the protein are positive with close values of 33 and 35 $Å^2$, respectively, but, the large R values of 16.9 and 16.4 for both the asymmetric and symmetric models reflect the poor agreement between theoretical and experimental SAXS profiles. Such lack of agreement between theoretical and experimental curves, especially at low Q values, Figure 5(a), may reflect the absence of internally bound water molecules within these submicellar models just as four internally bound water molecules were necessary to obtain the best R value of 0.0731 for the BPTI structure.

With this in mind, 120 water molecules were energy minimized and docked within the κ-casein cavity for both the asymmetric and symmetric submicellar structures. This cavity within the κ-casein molecule would in reality either contain either bound or free water. Bound water was chosen since 120 bound waters would mimic the amount of bound water determined via DNMR Relaxation results (5, 6), i.e., 0.007 g water/g protein, assuming all bound water fell within this cavity.

Subjecting these low hydrated structures (120 water molecules) to the Lattman method yielded good results with more acceptable R values of 0.682 and 0.611 for the asymmetric and symmetric models, respectively (Table 5). Also, the corresponding B_P values are both positive, i.e., 43 $Å^2$ whereas the B_W are both negative, -540 $Å^2$. The negative B_W values could be an artifact of the approximation by Lattman for positioning of the free water molecules at the same position as the protein and bound water atoms.

To follow the methodology developed with BPTI study, we now add a larger surface of water, i.e., 2703 water molecules to each of the low bound water submicelle structures using the droplet algorithm. This amount of water, 2823 moles water/mole protein, would mimic an accepted hydration value of 0.244 g water/g protein for globular proteins. The normal hydrodynamic hydration value for casein submicelles is on the order of 2 to 3 g water/g protein (13, 24), while the gravimetric hydration of isoelectric casein is about 0.7 g water/g protein (13, 15). However, due to the large number of water molecules involved to achieve these numbers as well as the length of the calculation, it would seem prudent to first attempt to solve the 2823 water molecule structure to ascertain if any improvement is observed in the R values. Using the Lattman procedure on the two droplet structures (i.e., asymmetric and symmetric + 2823 water molecules), which we shall define as high hydration structures, R values were obtained that were twice as large as those found when using the low hydration (120 water molecules) structures (see Table 5). Both B_P values for the asymmetric and symmetric high hydration structures were 36 $Å^2$ and in close agreement with the value of 43 $Å^2$ obtained using the low hydration structure. However, as in the BPTI study, the B_W values were now positive and the B_B values were more realistic, i.e., on the order of 100 $Å^2$. Hence, it would appear that the true hydration value for the submicellar casein structure lies somewhere between 120 and 2823 molecules of water per molecule of protein. The exact amount and location of these new bound waters can not be determined at this time. Further studies may, in time, resolve this problem.

We next energy minimized all four hydrated complexes, i.e., the low and high hydrated asymmetric and symmetric models, to further mimic the BPTI study, and subjected all four hydrated energy minimized structures to the Lattman procedure. Interestingly little improvement in fit occurred following the minimization of the protein water complexes (Table 5). The energy minimized theoretical and experimental profiles for the low and high hydrated structures are shown in Figures 5(b) and 5(c), respectively for comparison. In both figures the experimental data are given as filled triangles with connecting lines while the SAXS profiles that form the asymmetric and symmetric models are circles and squares, respectively. Figure 5(c) shows clearly that a less acceptable fit to the experimental data is obtained with both high hydrated structures, especially at low Q values. The zero Q value from which the molecular weight is calculated yields an acceptable value with the experimental value but all other Q values deviate significantly in a positive then a negative manner to a Q value of 0.05 $Å^{-1}$. Such a non-monotonic curve with a maximum at low Q values is indicative of high virial or ordering effects. Since this ordering is not observed in the experimental data, it appears that the droplet

Table 5. Temperature factors for submicelle structures from SAXS

Structure	Water	B_P	B_W	B_B	R
Asymmetric	None	33	-181	—	16.9
Asymmetric	Low	43	-540	413	0.682
Asymmetric	High	36	53	98	1.17
Symmetric	None	35	25	—	16.4
Symmetric	Low	43	-540	503	0.611
Symmetric	High	36	57	130	1.26
Asymmetric*	Low	46	-550	436	0.684
Asymmetric*	High	30	85	156	1.81
Symmetric*	Low	45	-550	500	0.612
Symmetric*	High	31	27	100	1.29

*Denotes energy minimized submicelle-water complex.
Note: All other parameters defined in Table 4.

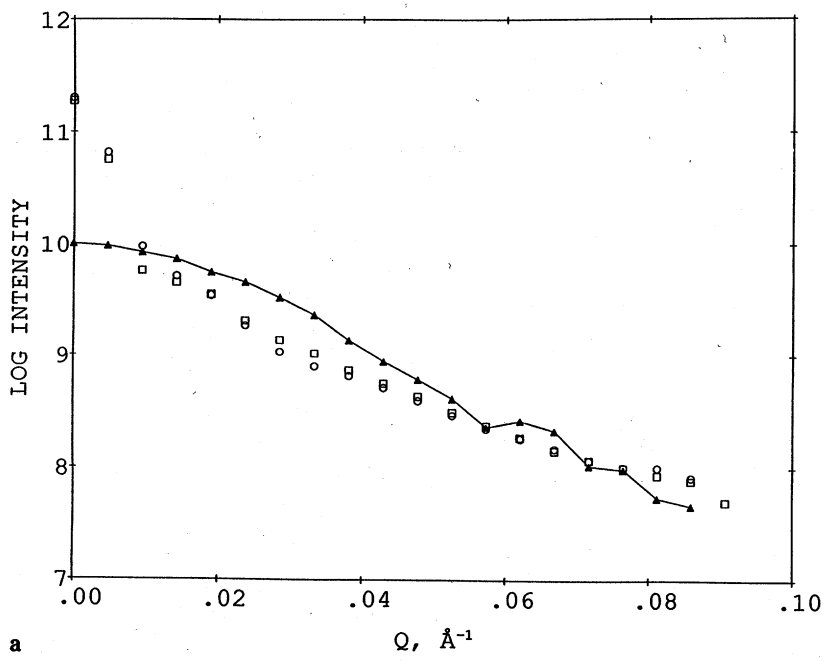

Figure 5. SAXS profiles of submicellar casein; solid triangles (▲) with connected lines represent experimental data (24). (a) Theoretical optimized curves from unhydrated asymmetric (circles) and symmetric (squares) energy minimized structures.

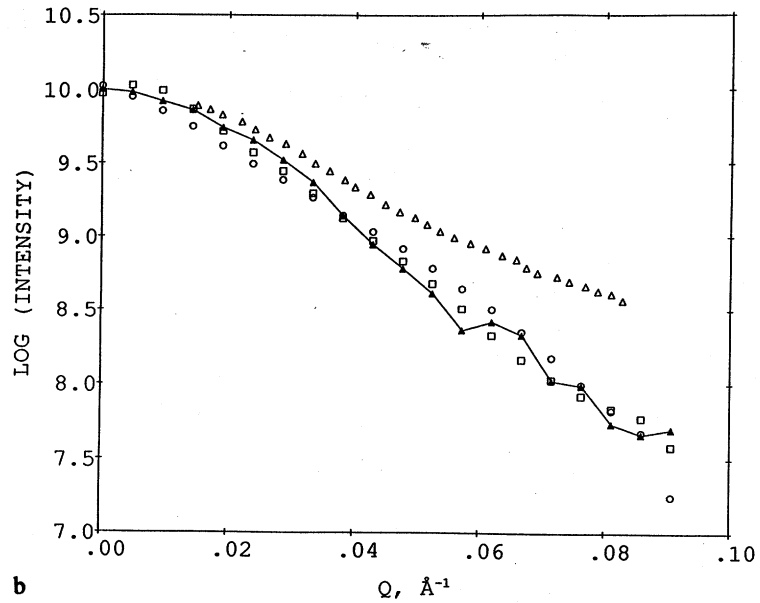

b

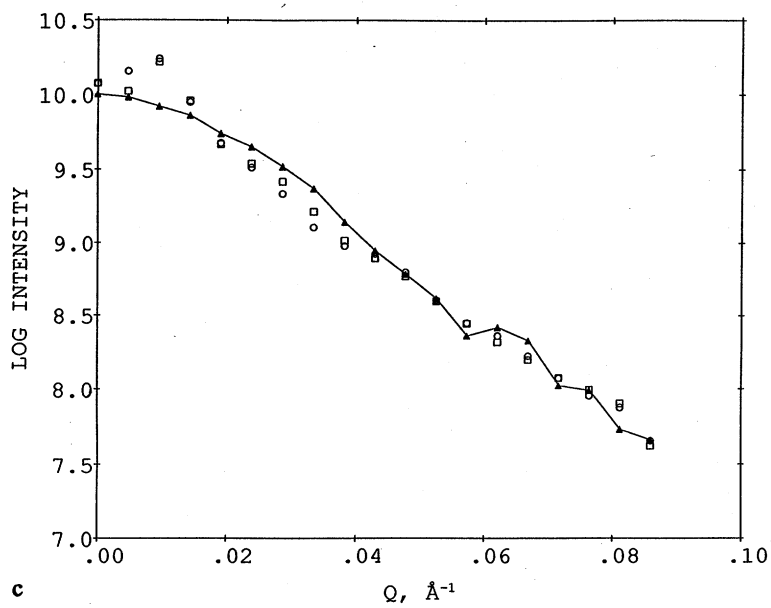

c

Figure 5. Continued. SAXS profiles of submicellar casein; solid triangles (▲) with connected lines represent experimental data (24). (b) Theoretical optimized curves of energy minimized low hydration (120 waters) asymmetric (circles) and symmetric (squares) structures; open triangles (Δ) are experimental small-angle neutron scattering in D_2O (38). (c) Theoretical optimized curves for energy minimized high hydration (2823 waters) asymmetric (circles) and symmetric (squares) structures.

water added to the low hydrated structures is not tightly bound water but are most likely free waters and easily exchanged with the bulk solvent molecules.

Figure 5(b) shows good agreement with theoretical and experimental SAXS profiles. Here, it can readily be seen that the circles are closer to the filled triangles than the squares which represent the SAXS profile calculated from the low hydrated asymmetric structure at almost all Q values. This fit is further reflected in Table 5 by a slightly lower R value of 0.612 for the low hydrated symmetric structure than the corresponding asymmetric model, 0.684. However, these results should indicate only that the low hydrated symmetric structure has only a slightly higher probability of existence in solution. These calculations and experiments do not justify the elimination of a symmetric form. What can be also concluded from this study is that the casein submicelle is structurally more rigid than globular proteins but overall more flexible, in that submicelle formation may occur under a variety of conditions with varying combinations of monomers (12). This is seen by the fact that the B_P values for all submicellar casein models yield values on the order of 35 to 40 $Å^2$ (Table 5), while the BPTI values were much higher, i.e., 135 to 200 $Å^2$ (see Table 4). These consistently lower B_P values for casein may be ascribed to the existence of proline residues throughout the polypeptide chain which would yield an open but more rigid structure. Conversely the movement of β-casein in and out of the complex with temperature is most likely not microscopically reversible (12).

In addition, the reported neutron scattering data of casein in D_2O (38) is shown in Figure 5(b) as open triangles. Here, the neutron data were normalized at zero Q value to be compared with the SAXS profiles. As can easily be observed, large differences exist between experimental SAXS profiles and neutron scattering data in D_2O. Whether this difference is a direct result of structural changes induced by the addition of D_2O is not clear at this time. However, these results do suggest to the casein investigator that care must be taken to avoid the addition of D_2O in casein solutions.

Finally, because of the rigid structure of all submicellar structures, it would be prudent to ascertain if the protein structure had an influence on the structure of the water molecules within the various hydrated forms. Figure 6(a) shows these 120 added water molecules within the κ-casein cavity for the energy minimized low hydrated submicelle structure. Only the water, shown as "wire-frame" structure and the ribboned backbone of κ-casein are displayed. The dashed lines indicate the presence of all hydrogen bonds. It can be easily seen that a worm-like structure of the 120 water molecules is present within the energy minimized κ-casein cavity. This super structure of waters is obviously due to the influence of protein electrostatic interactions and resembles a solid distorted cylinder as seen by the space-fill model of these waters shown in Figure 6(b). Previous studies have shown that the κ-casein molecule exhibits a dipolar character (22). The protein dipolar character is apparently superimposed on the internal water molecules based upon their stability within the cavity following minimization (Figure 6a,b). Here, then, is a clear representation of the influence of protein structure and energetics on internal bound water structures. That the protein structures did not change when water was added and the complexes were energy minimized, further suggests

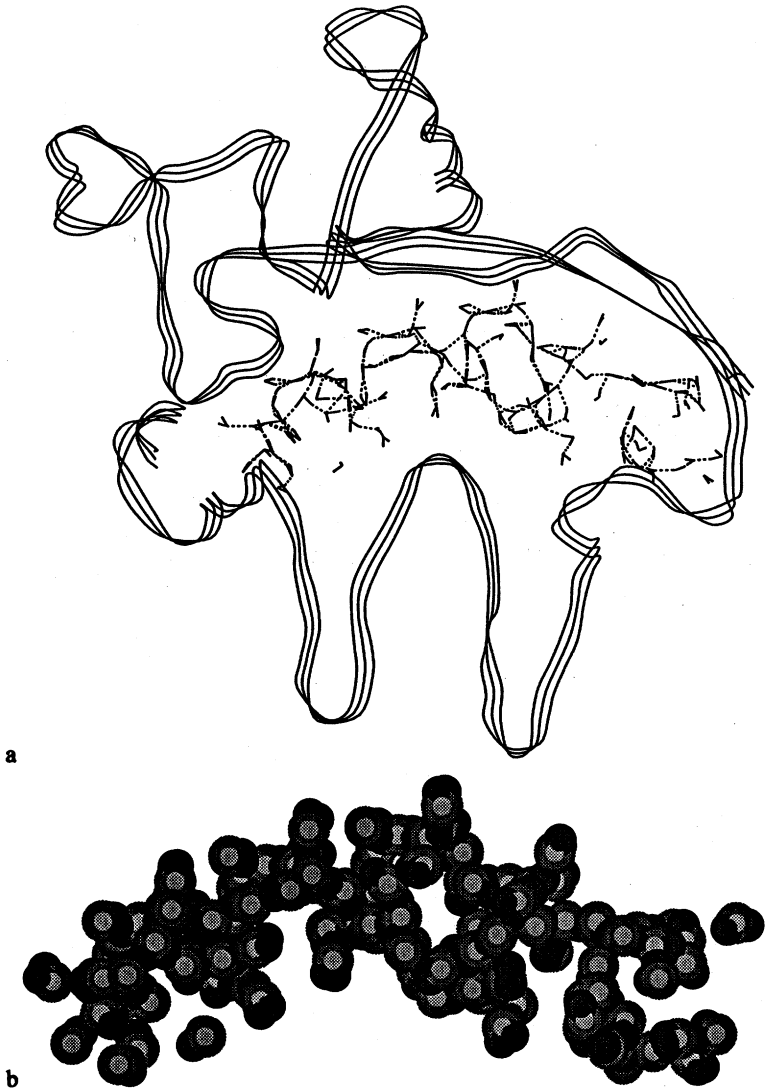

Figure 6. (a) Energy minimized docked low hydration waters (120 waters) displayed with ribboned κ-casein backbone structure; water in black v-shape, with dashed lines representing hydrogen bonding. (b) Space-filled energy minimized model of low hydration waters colored by atom types; oxygen in light to medium shading and hydrogen in dark to black shading.

the hypothesis that κ-casein, the backbone structure is somewhat rigid, while side chains have a great deal of mobility.

As emphasized in previous papers on the monomeric caseins (21-23), it must be kept in mind that these structures represent working models. They are not the final native structures but are presented to stimulate discussion and to be modified

as future research unravels the nature of these non-crystallizable proteins. Inspection of a recent drawing of the casein micelle by Holt (18) demonstrates how structures such as those presented here could be further aggregated into the casein micelle. Continued dialogue and research in this area may bring together the new concepts necessary to finally produce an accurate model. It is hoped that this work is a start in that direction.

Note

The mention of brand or firm names does not constitute an endorsement by the U.S. Department of Agriculture over others of a similar nature not mentioned.

Literature Cited

1. Ali, A. E.; A. T. Andrews; G. C. Cheeseman. *J. Dairy Sci.,* **1980,** *47,* 371-382.
2. Baldwin, R. L.; Yang, Y. T. In *Lactation: A Comprehensive Treatise,* Larson, B. L.; Smith, V. R. Eds. Academic Press Inc., New York, NY, 1974, p. 349-355
3. Berry, G. P.; Creamer, L. K. *Biochem.,* **1975,** *14,* 3542-3535.
4. Byler, D. M.; H. M. Farrell, Jr. *J. Dairy Sci.,* **1989,** *72,* 1719-1721.
5. Byler, D. M.; H. M. Farrell, Jr.; H. Susi. *J. Dairy Sci.,* **1988,** *71,* 2622-2629.
6. Clore, G. M.; Bax, A.; Wingfield, P. T.; Gronenborn A. M. *Biochem.,* **1990,** *29,* 5671-5676.
7. Creamer, L. K. *N.Z. J. Dairy Sci. and Technol.,* **1976,** *11,* 30-39.
8. Davies, D. T.; Law, A. J. R. *J. Dairy Res.,* **1980,** *47,* 83-90.
9. Davies, D. T.; Law, A. J. R. *J. Dairy Res.,* **1983,** *50,* 67-75.
10. Downey, W. K.; Murphy, R. F. *J. Dairy Res.,* **1970,** *37,* 361-372.
11. Eigel, W. N.; Butler, J. E.; Ernstrom, C. A.; Farrell, H. M., Jr., Harwalker, V. R.; Jenness, R.; McL. Whitney; R. *J. Dairy Sci.,* **1984,** *167,* 1599-1631.
12. Farrell, H. M., Jr. In *Fundamentals of Dairy Chemistry, 3rd Edition.* N. Wong, ed., Van Nostrand Reinhold, New York, NY, 1988, p. 461-510.
13. Farrell, H. M., Jr.; H. Pessen; Kumosinski, T. F. *J. Dairy Sci.,* **1989,** *72,* 562-574.
14. Farrell, H. M., Jr.; Kumosinski, T. F.; Pulaski, P.; Thompson, M. P. *Arch. Biochem. Biophys.,* **1988,** *265,* 146-158.
15. Farrell, H. M., Jr.; Pessen, H.; Brown, E. M.; Kumosinski, T. F. *J. Dairy Sci.*, **1990,** 73:3592-3601.
16. Gelin, B. R.; Karplus, M. Biochem. **1979,** *18,* 1256-1259.
17. Groves, M. L.; Dower, H. J.; Farrell, H. M.; Jr., *J. Protein Chem.,* **1992,** *11,* 21-28.
18. Holt, C. *Adv. in Prot. Chem.,* **1992,** *43,* 63-113.
19. Holt, C.; Sawyer, L. *J. Chem. Soc.,* **1993,** *89,* 2683-2690.
20. Kumosinski, T. F.; Farrell, H. M., Jr. Calcium-induced associations of the caseins: thermodynamic linkage of calcium binding to colloidal stability of casein micelles. J. Protein Chem. **1991,** *10*, 3-11.
21. Kumosinski, T. F.; Brown, E. M.; Farrell, H. M., Jr. *J. Dairy Sci.,* **1993,** *76,* 931-945.

22. Kumosinski, T. F.; Brown, E. M.; Farrell, H. M., Jr. *J. Dairy Sci.,* **1993,** *76,* 2507-2520.
23. Kumosinski, T. F.; Brown, E. M.; Farrell, H. M., Jr. In *Molecular Modeling. ACS Monograph Series,* Kumosinski, T. F.; Liebman, M. N., eds. Denver, CO, 1994.
24. Kumosinski, T. F.; Pessen, H.; Farrell, H. M., Jr.; Brumberger, H. *Arch. Biochem. Biophys.,* **1983,** *266,* 548-561.
25. Kyte, J.; Doolittle, R. F. *J. Mol. Biol.,* **1982,** *157,* 105-132.
26. Lattman, E. E. *Prot. Stru, Funct. and Gene.* **1989,** *5,* 149-158.
27. Lin, S. H. C.; Leong, S. L.; Dewan, R. K.; Bloomfield, V. A.; Morr, C. V. *Biochem.,* **1972,** *11,* 1818-1821.
28. Noble, R. W., Jr.; Waugh, D. F. *JACS,* **1965,** *87,* 2236-2242.
29. Otting, G.; K. Wüthrich. 1989. Studies of protein hydration in aqueous solution by direct NMR observation of individual protein-bound water molecules. J. Am. Chem. Soc. *111,* 1871-1875.
30. Pepper, L., *Biochim. Biophys. Acta* **1972,** *278:* 147-155.
31. Pepper, L.; Farrell, and H. M., Jr. Interactions leading to formation of casein submicelles. *J. Dairy Sci.,* **1982,** *65,* 2259-2266.
32. Pessen, H.; Kumosinski, T. F.; Farrell, H. M., Jr.; Brumberger, H. *Arch. Biochem. Biophys.,* **1991,** *284,* 133-142.
33. Pickover, C. A.; Engleman, D. M. On the interpretation and prediction of X-ray scattering profiles of macromolecules in solution. Biopolymers 21:817-828.
34. Rose, D. *J. Dairy Sci.,* **1968,** *51,* 1897-1902.
35. Schmidt, D. G.; Payens, T. A. J. In *Colloidal aspects of casein in surface and colloid science, Vol. 9.* E. Matijevic (Ed.). Wiley and Sons, Incorp. New York, NY. 1976.
36. Schmidt, D. G. In *Developments in Dairy Chemistry* -1, P. F. Fox (Ed.). Applied Science Publish Limited, Essex, England, 1982, p. 61-93.
37. Slattery, C. W.; Evard, R. *Biochim. Biophys. Acta.,* **1973,** *317,* 529-538.
38. Stothart, P. H. *J. Mol. Biol.* **1989,** *208,* 635-639.
39. van de Vroot, F. R.; Ma, C.-Y.; Nakai, S. *Archives Biochem. Biophys.* **1979,** *195,* 596-603.
40. Vreeman, H. J.; Brinkhuis, J. A.; Van Der Spek, C. A. *Biophys. Chem.* **1981,** *14,* 185-193.
41. Walstra, P. *J. Dairy Sci.* **1990,** *73,* 1965-1979.
42. Waugh, D. F.; Von Hippel, P. H. *J. Am. Chem. Soc.* **1956,** *78,* 4576-4582.
43. Waugh, D. F.; Creamer, L. K.; Slattery, C. W.; Dresdner, G. W. *Biochem.,* **1970,** *9,* 786-795.
44. Weiner, S. J.; Kollman, P. A.; Case, D. A.; Singh, U. C.; Ghio, C.; Alagona, G.; Profeta, S.; Weiner, P. *J. Am. Chem. Soc.,* **1984,** *106,* 765-784.
45. Weiner, S. J.; Kollman, P. A.; Nguyen, P. T.; Case, D. A. *J. Comput. Chem.* **1986,** *7,* 230-252.
46. Woychik, J. H.; Kalan, E. B.; Noelken, M. E. *Biochem.* **1966,** *5,* 2276-2288.

This color plate is for Chapter 22.

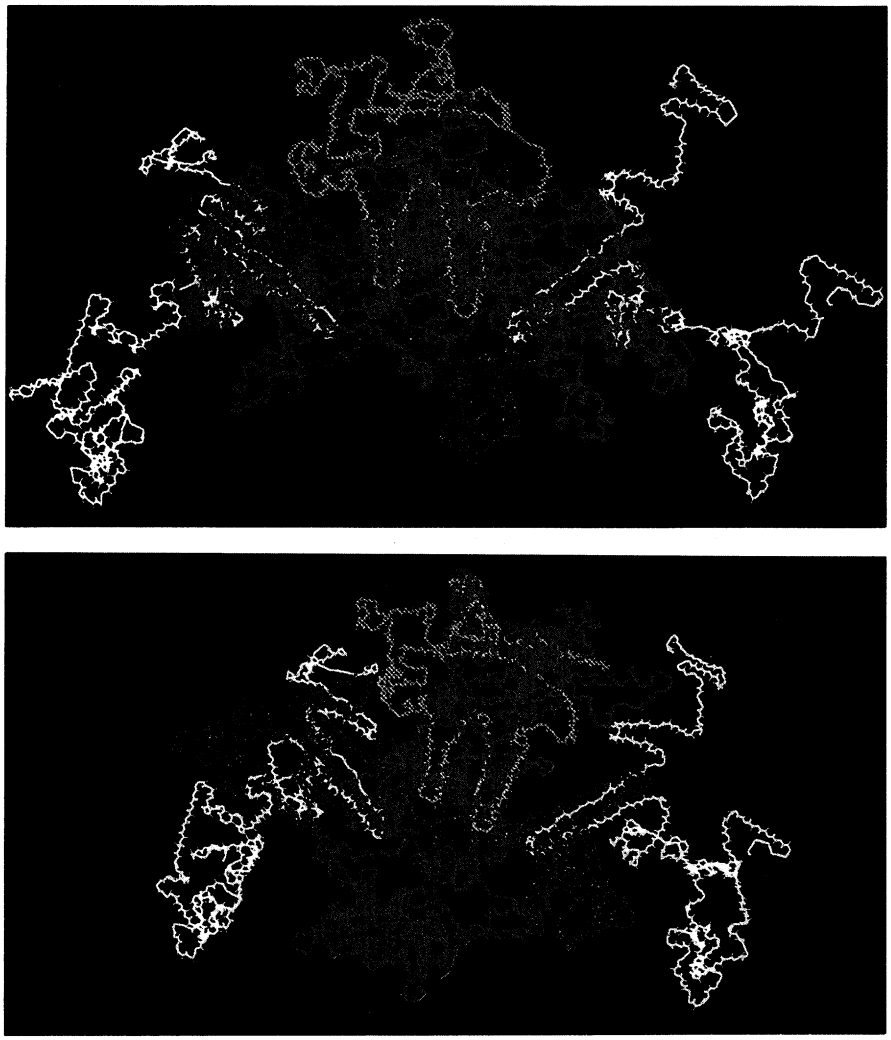

Color Plate 20. (Top) Energy minimized casein asymmetric submicelle structure, i.e., one $\varkappa$-casein B, four α_{s1}-casein B and two β-casein A^2 asymmetric dimers. Ribboned backbones without side chains; $\varkappa$-casein B in cyan, α_{s1}-casein B in red and white; β-casein A^2 backbone colored in magenta. (Bottom) Energy minimized casein symmetric submicelle structure, i.e., one $\varkappa$-casein, four α_{s1}-casein B and two β-casein symmetric dimers. Ribboned backbones without side chains; $\varkappa$-casein B in cyan, α_{s1}-casein B in red and white β-casein A^2 in magenta.